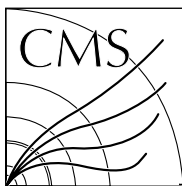


Available on CMS information server

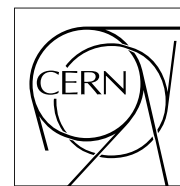
CMS NOTE-2006/052



The Compact Muon Solenoid Experiment

# CMS Note

Mailing address: CMS CERN, CH-1211 GENEVA 23, Switzerland



April 26, 2006

## CMS Preshower *in-situ* Absolute Calibration with Physics Events

Ioannis Evangelou

*Univ. of Ioannina, Physics Dept., IOANNINA, 45110-GREECE**ECAL Group*

### Abstract

This note describes the *in-situ* absolute calibration of the Preshower detector of CMS. The Preshower is based on silicon strip sensors that will be installed in the endcaps of CMS in front of the crystal Calorimeter. Energy deposited in the lead of the Preshower is estimated by the silicon sensors, allowing a re-scaling of the energy measured by the endcap crystals. Measurement of the energy deposited in the lead absorbers to 5% accuracy is required over a very large dynamic range (1-400 MIPs equivalent), thus a maximum accuracy of 1% on the measurement of the charge deposited in the silicon will be sufficient. There are two principle sources of response variation at startup (sensor-to-sensor and channel-to-channel): sensor thickness (RMS of 1-2%) and gain uniformity of the electronics (RMS ~3%). These will be measured and thus taken into account. Radiation damage to the sensors (decrease in charge collection efficiency by up to 17% over 10 years) and the electronics (decrease in gain by up to 2% over 10 years) will need to be assessed by periodic *in-situ* calibrations. A precise *in-situ* absolute calibration using minimum ionizing particle signals from physics events is examined. For the calibration method the full simulation framework of CMS has been used (CMSIM/CMKIN, OSCAR and ORCA). It is shown that sufficient calibration accuracy can be obtained by using muon or pion events, and that the time required for the calibration is of the order of a few days at initial LHC luminosity and at least a factor of two less for nominal LHC luminosity.

# 1 Introduction

The aim of this work is to simulate full physics events, in the presence of pileup, select MIPs (minimum ionizing particles) in the Preshower region and attempt to see the single MIP signals. The time necessary for the absolute calibration can then be estimated especially for low luminosity running (the most demanding case). It is assumed that electronics and geometrical effects are already taken into account (calibrated) prior to data taking operation. This note concentrates most on effects on sensors (decrease in charge collection efficiency) and electronics (decrease of gain) from radiation damage - i.e. *in-situ* calibration.

A short description of the Preshower detector is presented followed by the front-end electronics and the Internal Calibration Circuit. Then, the calibration procedure is explained with the analysis method to select MIPs and their deposited energies in the Silicon Sensors. Two approaches are examined for the MIP distributions: a) use of reconstructed muons in physics events and b) use of reconstructed pions in physics events. The selection criteria and the results are presented. Finally the performance of the calibration procedure is evaluated and the time needed for full Preshower calibration at a module basis is estimated.

## 2 The Preshower of CMS

A global view of the Preshower (ES) in the upper half of one endcap is shown in fig.1 [1]. It contains two planes of silicon strip sensors, with their strips arranged vertically ('X' plane, closest to interaction point) and horizontally ('Y' plane) respectively. Each 320  $\mu\text{m}$  thick sensor contains 32 strips of 1.9 mm pitch and is mounted together with a front-end hybrid on a ceramic support and an aluminum tile to form a "micromodule". The total number of sensors is approximately 4300, corresponding to around 138000 total channels. Two lead absorbers of radiation lengths 1.9 $X_0$  and 0.9 $X_0$  for normal incidence are placed in front of the X and Y planes respectively. Their purpose is to initiate photon showers, in order to facilitate  $\gamma/\pi^0$  discrimination (the main purpose of the ES) without degrading too much the energy resolution of the crystal calorimeter. Also shown in fig.1 is the arrangement of the "ladders" that house the micromodules for the first plane ('X') of the ES.

The front-end electronics (section 3) measure the energy deposited in the ES sensors, normally expressed in terms of MIPs. One MIP is defined as the most probable energy deposited by a high energy particle traversing 320 $\mu\text{m}$  (the nominal thickness of the ES sensors) of silicon. It is equivalent to about 83.7keV for normally incident particles (i.e. muons with  $p_\mu \approx 0.5\text{GeV}/c$ ), or, expressed as an equivalent charge deposit, 3.7fC.

The actual energy measured by one of the ES sensors due to the passage of a high energy charged particle depends upon many factors: the angle of incidence (hence the precise thickness of silicon traversed), the energy of the particle and the particle type, as well as applied thresholds and statistical errors. Most of the signal distributions presented in this note are inclusive on all ES micromodules. It is therefore difficult to claim absolute numbers: we concentrate more on the proof of principle. It should also be noted that the thickness of silicon in the simulation packages used up to now was actually 300 $\mu\text{m}$  and not the nominal 320 $\mu\text{m}$ .

The total deposited energy in the ECAL+ES system is given by  $E = E_g + E_{\text{presh}}$  where  $E_g$  is the energy measured by the ECAL and  $E_{\text{presh}} = \gamma(E_X + \alpha E_Y)$  in MIP units is the energy measured by the ES.  $E_{X,Y}$  are the deposited energies in the planes X and Y of the ES respectively,  $\alpha$  is the relative weight of the two planes and  $\gamma$  is the slope of the  $E_g[\text{GeV}] = f(E_X + \alpha E_Y)[\text{MIPs}]$  plot, which effectively relates the energy deposited in the lead to that measured by the silicon sensors. Typical values of  $\alpha = 0.6-0.8$  and  $\gamma = 0.024[\text{GeV}/\text{MIP}]$  have been evaluated from beam test data [2] and simulation.

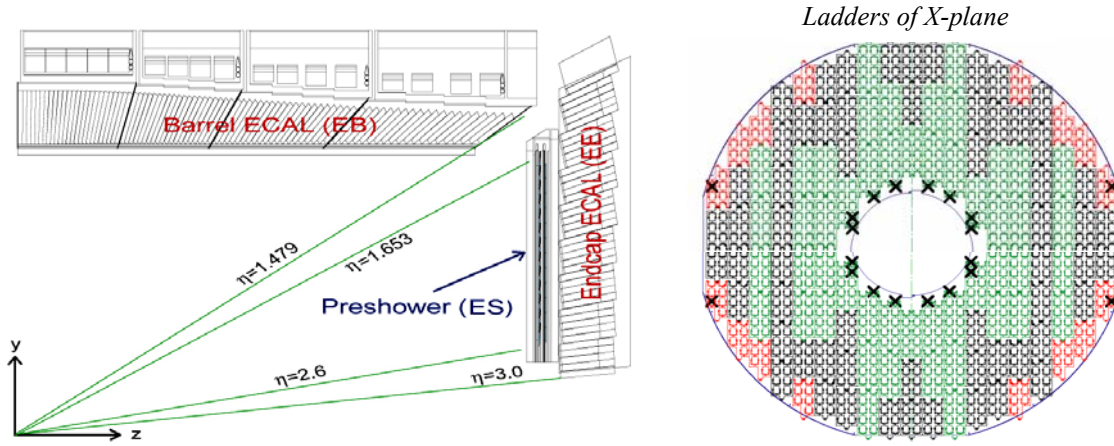


Figure 1. The Preshower detector in front of the endcap ECAL

### 3 The Internal Calibration Circuit

The readout electronics of the ES have a large dynamic range in order to measure the energy deposited by very high energy electron/photon showers. In normal running the maximum charge in a single strip that can be measured (without causing overflows) is equivalent to about 400 MIPs. The  $\gamma/\pi^0$  separation relies upon transverse shower shape analysis, requiring the measurement of small signals with a relatively tight threshold cut, of not more than one or two MIPs.

The front-end electronics are organized as an analogue pipeline, where events are stored in a front-end ASIC called PACE3 (one PACE3 per sensor – fig.2) [3], followed by an on-detector analogue to digital conversion stage and a non-zero-suppressed data transmission system to the counting room. For each event the PACE3 outputs 3 voltage samples per channel at a rate of 20MHz. A 40MHz ADC [4] converts the samples with 12-bit precision, the data then being transmitted to the K-chip [5] for data concentration, packaging and subsequent transmission via optical link to the off-detector readout electronics.

PACE3 is actually an assembly of two chips merged to one package: a low noise preamplifier and shaper (Delta3) optimized to be used on high capacitance silicon strip sensors and a 192 locations deep analogue memory (PACE-AM) used to store the signal samples while waiting for the Level-1 (L1) trigger to arrive, with an output multiplexer. PACE3 can operate in two modes: Low Gain (LG) for normal running with a large dynamic range (specification: 1 to 400 MIPs with a S/N ratio for single MIPs of  $\sim 2$ ) and High Gain (HG) for calibration purposes (specification: 0.1 to 50 MIPs, with a S/N ratio for single MIPs of  $\sim 9$ , fig.3).

The output of PACE3 may not be a linear function of the charge deposited in the silicon, and may also vary from channel to channel (and PACE3 chip to chip). In order to measure the linearity, and to compare channels/chips, PACE3 incorporates an internal calibration circuit (ICC, the “calibration” box in the Delta chip of fig.2). An 8-bit internal DAC called VoCal provides precise voltage pulses on any selected channel (or combination of channels) through capacitors (one per channel). The injection capacitors have a nominal value of 1.275pF, with a variation in value significantly less than 1% within a PACE3. This variation has been calculated taking into account the parasitic capacitors and chip foundry specifications. A VoCal voltage of 2.9mV provides a charge into the preamp equivalent to 3.7fC (1 MIP). The ICC may operate in two modes: High Precision (HP) and Low Precision (LP). The HP operation of the ICC provides voltage pulses in the range of about -32mV to 26mV with a step of  $lsb=0.3mV$ . This corresponds to approximately -11 to 9 MIPs with  $lsb=0.1$  MIP. The LP operation provides pulses in the range of -39mV to 1.25V with an  $lsb=7.0mV$ . This corresponds approximately to -13 to 430 MIPs with an  $lsb=2.4$  MIPs (fig.4).

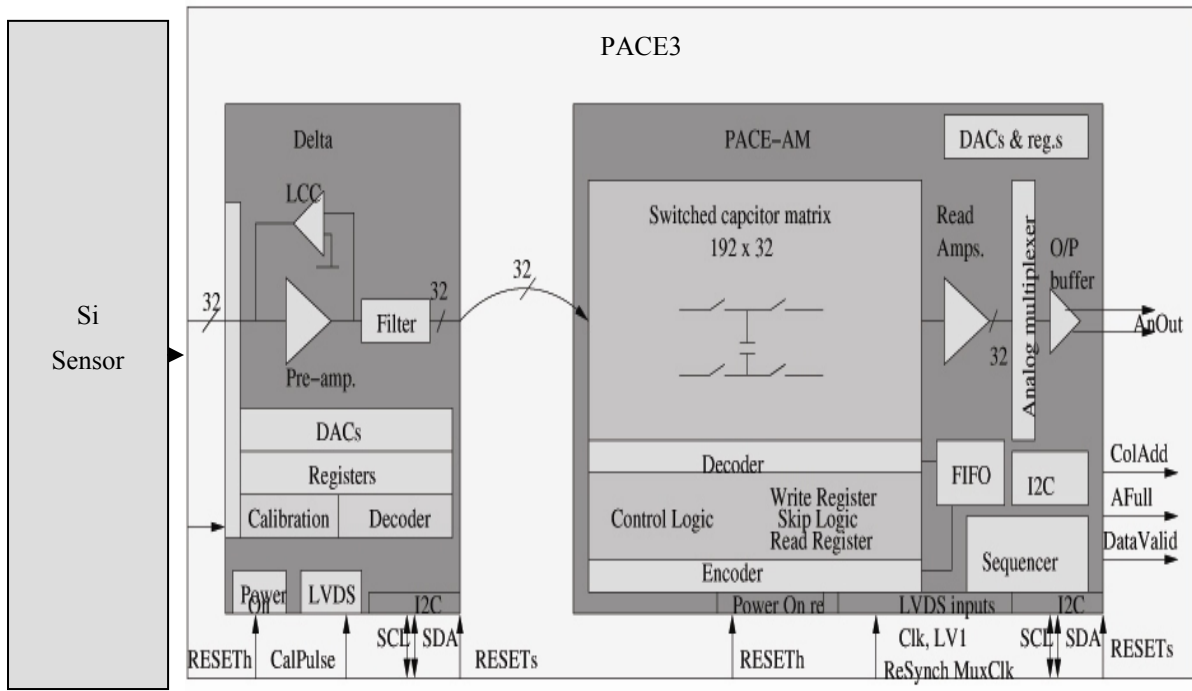


Figure 2. Front-End Readout System (Si Sensor and PACE3)

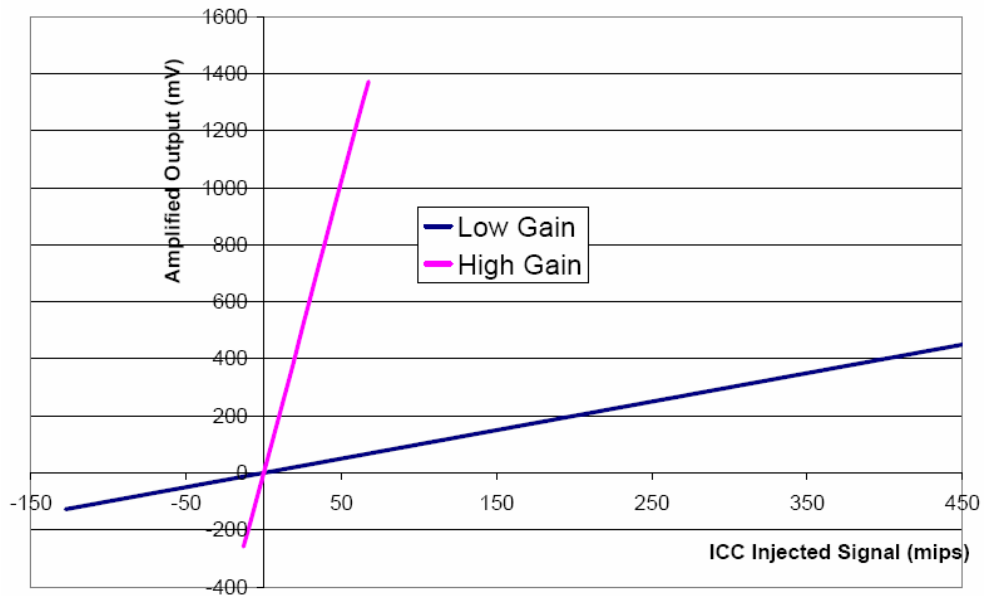


Figure 3. PACE3 Calibration: Overlap between the two gains

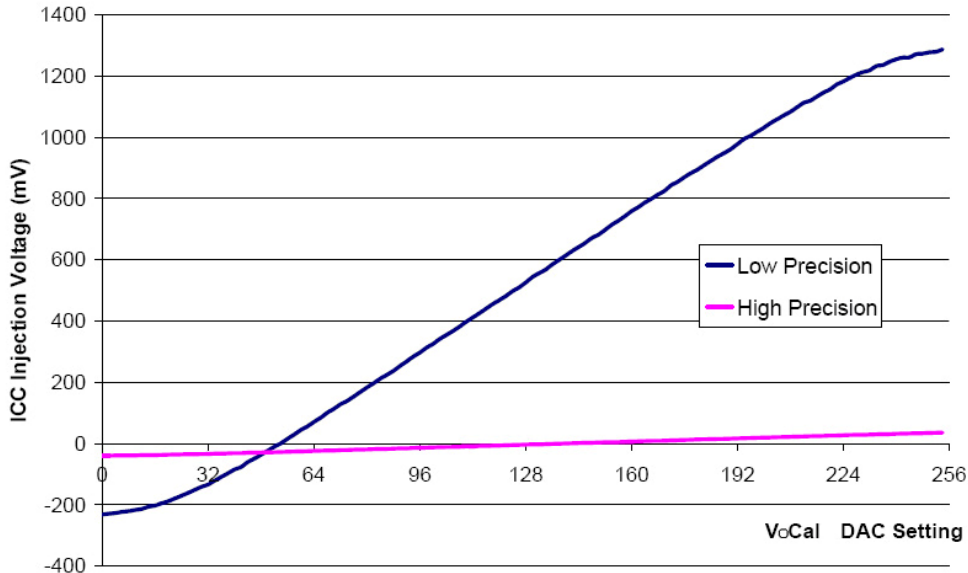


Figure 4. PACE3 Calibration: Response from the calibration circuit

In principle the ICC could be used to perform channel-channel and chip-chip calibrations. However, there are two limiting factors:

- Although the injection voltage can be accurately measured *in-situ*, using DCU (detector control unit, [6]) chips mounted on the front-end hybrids, the capacitance of the injection capacitor cannot be measured, and may vary between channels and between chips, due to fabrication uncertainties. Thus the exact charge injected can vary. This variation is estimated to be of the order of a few percent (maximum) between chips, and significantly less than 1% within a single chip.
- The “MIP” signal in the silicon sensors varies with pseudorapidity (due to incidence angle, which will be accounted for offline) and time: radiation damage to the silicon affects the charge collection efficiency – an effect up to 17% over the 10 year lifetime of LHC at the highest pseudorapidity [7].

In consequence, the internal injection pulse must itself be calibrated. The idea is that real minimum ionizing particles can be used for this purpose.

## 4 The Calibration Procedure

In CMS MIPs can be approximated by high energy muons and/or charged pions. The occupancy in the preshower is rather low, around 0.2% on average at low luminosity. Noise is thus the dominant “signal” in the strips, necessitating the use of the tracker and/or muon chambers to point to strips that have been traversed. The idea is to match the peak of a well defined real MIP distribution of the selected tracks, with the PACE in HG mode (fig.5, step 1), to the amplitude of an internal injection circuit, by setting the DAC accordingly in HP (Absolute MIP Calibration). The zero point is also determined (zero amplitude output for the internal charge injection) by setting the DAC accordingly. These are the only absolute points that can be determined. These two points allow the determination of “number of MIPs per DAC step” for the HP mode (“nMIPsPerDAC\_HP”). The DAC will then be set to a high value (e.g. 250, fig.5, step 2) and the corresponding number of MIPs estimated (which is expected to be around 10 MIPs, “nMIPsMax\_HP”). The injection precision will then be changed to LP (fig.5, step 3), and the DAC value adjusted to obtain the same output amplitude as nMIPsMax\_HP. The zero point will again be found in LP, allowing the estimation of “nMIPsPerDAC\_LP”. The DAC will then be set to a high value (without saturating the output, e.g. equivalent to about 50 MIPs, fig.5, step 4) and “nMIPsMax\_LP” found. Finally, the gain of the PACE3 is changed to LG (normal running mode). This full procedure is illustrated in fig.5. As the number of MIPs input by the internal injection has now been calibrated, the absolute gain and variation with input charge (linearity) in LG can be determined.

In fig.6 a typical muon energy spectrum from the 2004 testbeam runs is shown [8]. A muon beam of  $E_\mu=150\text{GeV}$  was directed to an ES micromodule (strip 15) with  $15^\circ$  impact angle. It is seen that the MIP peak is sitting at 48 ADC counts. With the PACE3 in HP the VoCal DAC is set accordingly to match zero and 48 ADC counts

respectively. The difference of the two VoCal settings will define the VoCal value equivalent to a MIP signal in HP.

The requirements during normal data taking or during special calibration runs (including a pre-calibration of each micromodule with cosmic rays prior to installation of the ES in CMS) of the detector will be to obtain a well defined signal distribution of real MIPs. This will be done at the initial ES operation and every year at the beginning of the data taking period. It may have to be repeated periodically due to radiation damage to the silicon. Strip by strip calibration is not necessary due to the small variation of the injection capacitors within a single chip – i.e. the ICC can be used to determine inter-channel calibration within a single micromodule. Thus a calibration at the level of micromodule with real MIP particles will be sufficient.

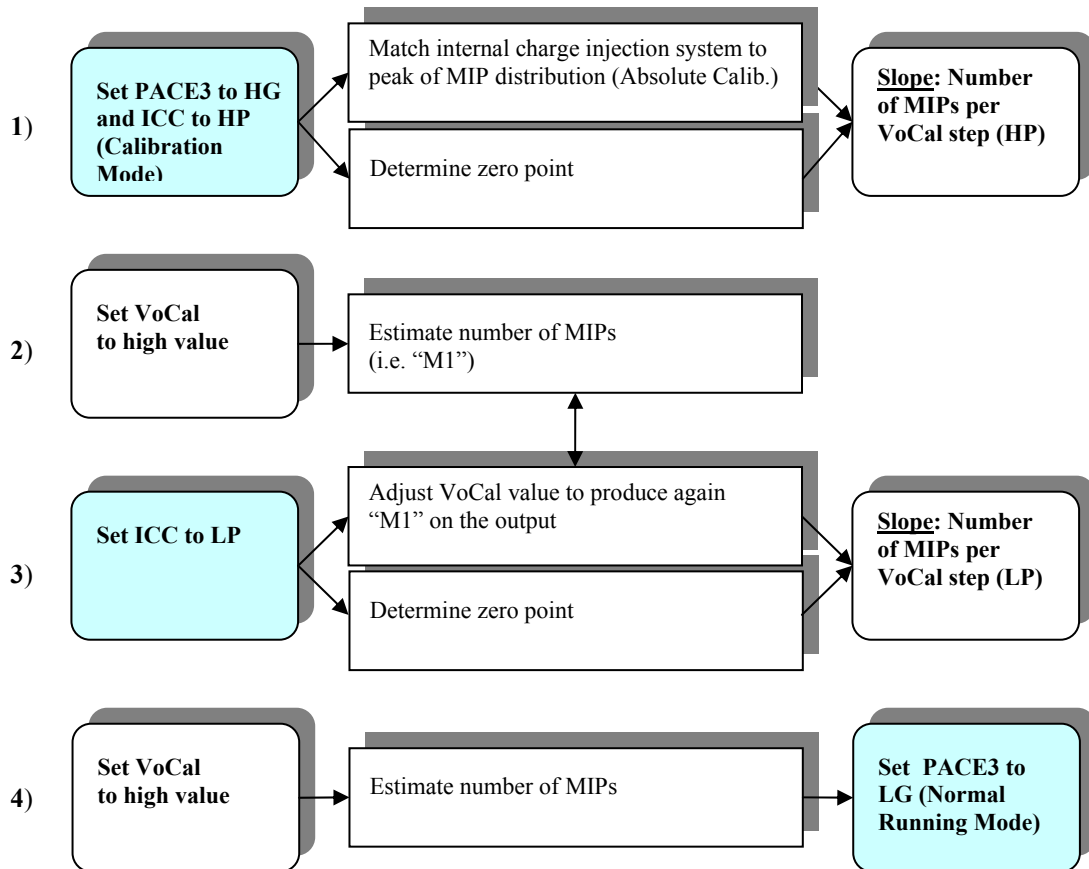


Figure 5. The Full Preshower Absolute Calibration Procedure

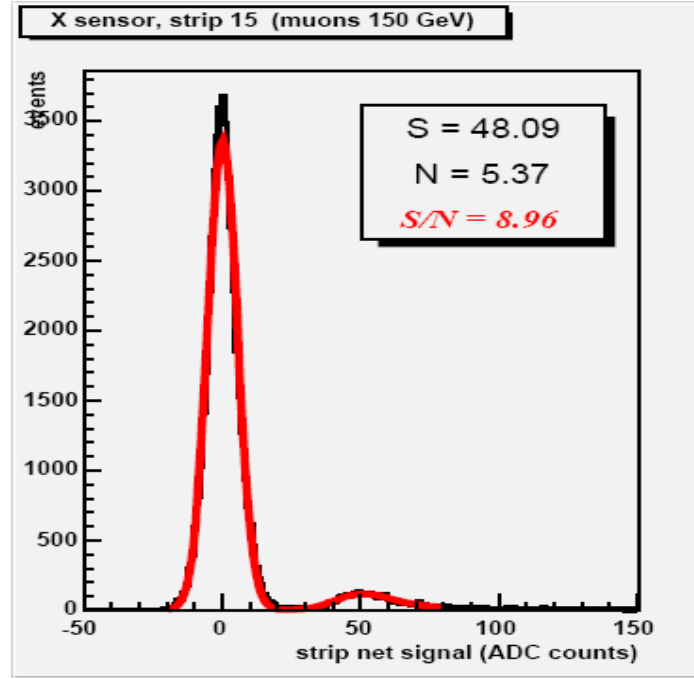


Figure 6. A typical Muon Energy Spectrum from the beam test run in 2004 ( $E_\mu=150\text{GeV}$ )

## 5 The Analysis Method

The PACE3 performs shaping of the signal from the silicon strips, with a peaking time of 25ns. The ideal pulse shape is approximated by the formula:

$$f(t) = \frac{Q_{cf} x_f^{(n-1)}}{(n-1)!} e^{-\omega_c t}$$

$$\text{With: } x_f = A \omega_c t$$

where:  $Q_{cf}$  is the charge delivered at the input divided by the input capacitance ( $Q_{cf}=Q/C_f$ ),  $A$  is the gain and  $n$  the order of the filter,  $\omega_c$  is the central frequency of the filter and is related to the peaking time  $\tau_p$  by:  $\omega_c=1/\tau_0 = n/\tau_p$ , with  $\tau_0$  the time constant of the filter. Typical values for an equivalent charge deposited of a MIP are:  $A=6.0$ ,  $n=3$ ,  $Q_{cf}=3.7 \times 10^{-15} \text{ C} / 350.0 \times 10^{-15} \text{ F}$ ,  $\omega_c=2.0/25.0 \text{ s}^{-1}$  and  $\tau_p=25 \text{ ns}$  [9,10]. With these values the corresponding pulse shape is shown in fig.7. The output of the shaper is continuously sampled at 25ns intervals. Upon reception of a Level-1 trigger, three consecutive samples are stored for subsequent readout. These samples occur at -5ns, 20ns and 45ns relative to the arrival of the trigger signal. The pedestal and energy calculations are obtained with a deconvolution method using the digitized samples with proper weights (fig.7, Table 1 [10]). Work is in progress on improving the method to parameterize the PACE3 pulse height as a function of the three time samples. The ES only measures a fraction of the original incident particle energy, and therefore, the noise is given in measured energy (before the sampling-fraction rescaling). For simulation purposes a Gaussian uncorrelated noise is included into each individual time sample. The standard deviation of the Gaussian noise distribution is set to  $15\text{keV}^1$  and the zero suppression thresholds to 54keV. The result of the above settings and simulations is to have for each event almost 1k strips out of the 138k with noise above threshold.

<sup>1</sup> Signal to noise for a single MIP signal in high gain mode has been measured to be around 9 in recent beam tests, corresponding to an equivalent noise of about 9keV. A safety factor of 50% is included in the simulation.

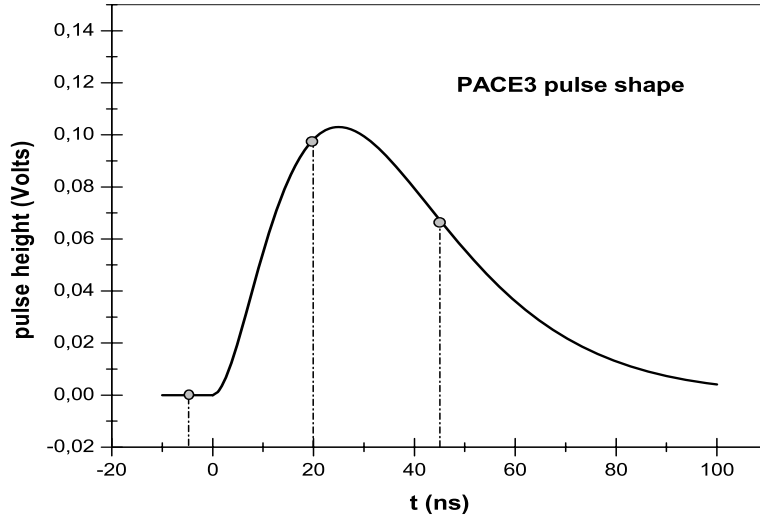


Figure 7. The PACE3 pulse shape with the three nominal voltage sampling points

Unit Pulse Shape	Energy Weight	Pedestal Weight
0.0	-1.1252	0.9368
0.9548	0.8780	-0.1375
0.6542	0.2472	0.2007

Table 1. The present parameterization of the pulse height in ORCA

The strip occupancy of the ES is relatively low – a fraction of a percent at low  $\eta$  and low luminosity, rising to a few percent at high  $\eta$  and high luminosity. This means that it is necessary to use tracks pointing to particular strips in order to obtain efficient MIP distributions. The CMS simulation framework [11] was used with two approaches:

- Muon tracks from inelastic physics events reconstructed with the “GlobalMuonReconstruction” algorithm of the CMS software packages. This is a standalone method using the muon chambers (RPCs & CSCs in the endcaps) to find its own “seed” or hit in the outer region. The muon trajectory is then evaluated by following the recorded hits all the way to the primary vertex with the “Kalman Filter” method using all muon chambers and full Tracker information. Cuts on the quality of the muon tracks reconstructed are applied at this stage: the normalized  $\chi^2$  of the muon track fit is required to be less than 1.5, which is at about  $2\sigma$  of the distribution (fig.9b). It should be noted that the fiducial coverage of the muon chambers extends only to  $|\eta| < 2.4$
- Charged pion tracks from minimum bias or jet events. Only tracker information is used for reconstruction with the “CombinatorialTrackFinder” method. Also here, reconstruction quality cuts are applied: the normalized  $\chi^2$  of the track fit in the tracker is required to be less than 2.0 (fig.15b). The CMS Tracker extends to  $|\eta| < 2.5$

The impact points of the reconstructed trajectories at the ES are stored for both planes ( $X$  and  $Y$ ) as well as the coordinates of the strips of the ES having signals above threshold. The impact point coordinates are then compared to all found “strips with signal” coordinates for each plane of the ES and in both directions (forward



and backward). A strict match is required for the first plane ( $|\Delta X(X\text{-plane})| < 0.12\text{cm}$  – i.e. close to strip pitch) and the same for the other coordinate, in the second plane ( $|\Delta Y(Y\text{-plane})| < 0.12\text{cm}$ ). Looser matches are required on the other coordinates (i.e.  $|\Delta Y(X\text{-plane})| < 3.05\text{cm}$  and  $|\Delta X(Y\text{-plane})| < 3.05\text{cm}$  respectively, corresponding to the strip length). This selection was checked and justified by the  $\Delta X$  and  $\Delta Y$  plots (fig.10) that show a flat distribution for the above limits. The tracks that have matched hits simultaneously in both planes are recorded and their deposited energies in the ES layers are added to the MIP distributions. A simplified diagram of the matching method is shown in fig.8.

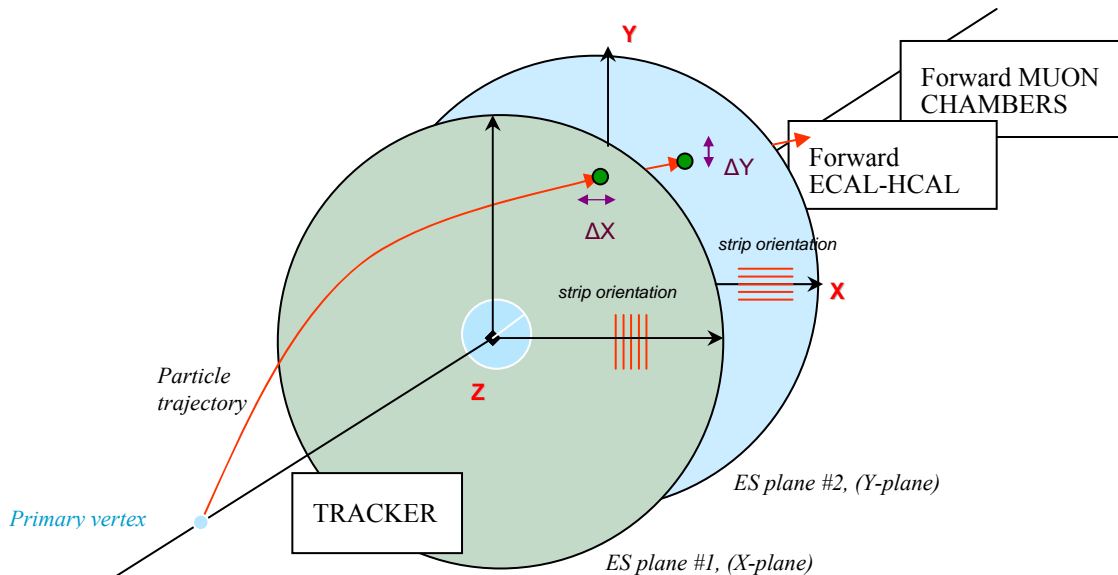


Figure 8. A simplified diagram of the matching between hits and signals in the ES planes

## 6 The MIP distributions of muons

In order to evaluate the code, first single muon track events were examined. Events, each with a single negatively charged muon with  $p_T=50\text{GeV}/c$  and flat pseudorapidity distribution in the range of  $|\eta| < 2.6$  were produced, simulated and digitized using the full CMS simulation framework (i.e. CMKIN\_3\_2\_0, OSCAR\_3\_3\_0 and ORCA\_8\_2\_0). The analysis code developed in ORCA\_8\_2\_0 was used to reconstruct and select muon tracks which traverse the ES and match strips with signal, in order to define the MIP distribution. The number of hits per track and the  $\chi^2$  distributions of the reconstructed tracks are shown in fig.9. To ensure a good reconstruction a cut of  $\chi^2/\text{ndf}$  at 1.5 is applied (equivalent to about  $2\sigma$ ), which reduces the selected tracks by about 28%. The impact coordinates of the muon tracks on the preshower layers are recorded and compared to the coordinates of strips having signal above threshold (i.e. 54 keV) as explained in the previous section. The distributions of  $\Delta X$  and  $\Delta Y$  for the first layer of Preshower in both directions forward and backward are shown in fig.10. Cuts on the strip area are applied on  $\Delta X$  and  $\Delta Y$  which represent the flat region of the distributions. Fig.11 shows the hit profile on both ES planes for the selected tracks. The red points represent the hits on ES #1 and the blue points the hits on ES #2. For flat pseudorapidity distributions the ES micromodules in the outer region (at the ring of the maximum radius of the disk) have much lower occupancy than the micromodules in the inner region closer to the beam pipe (ratio 1:7.4).

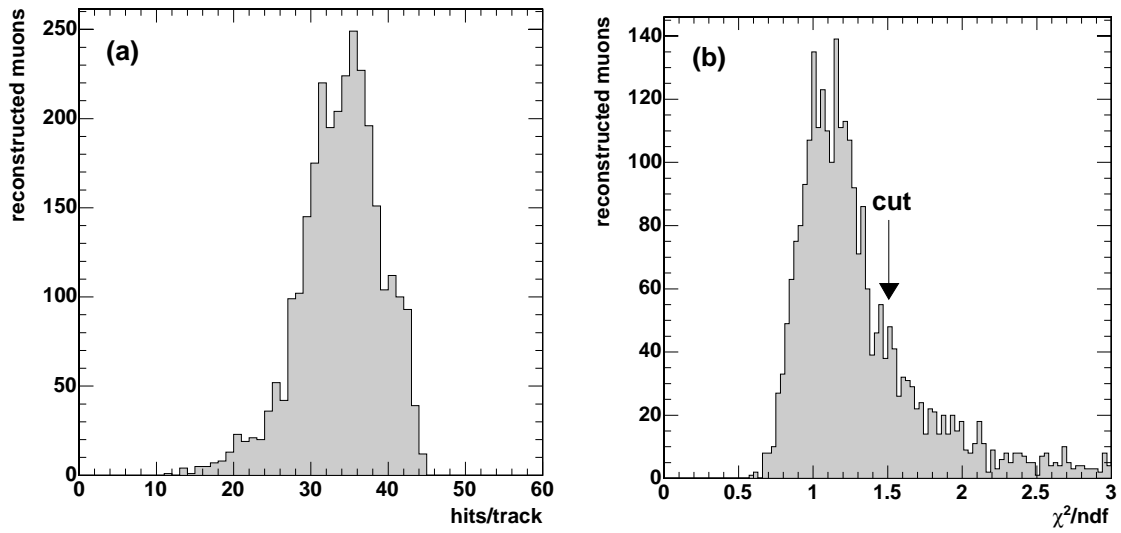


Figure 9. Number of hits per track (a) and  $\chi^2/\text{ndf}$  (b) of the reconstructed muon tracks

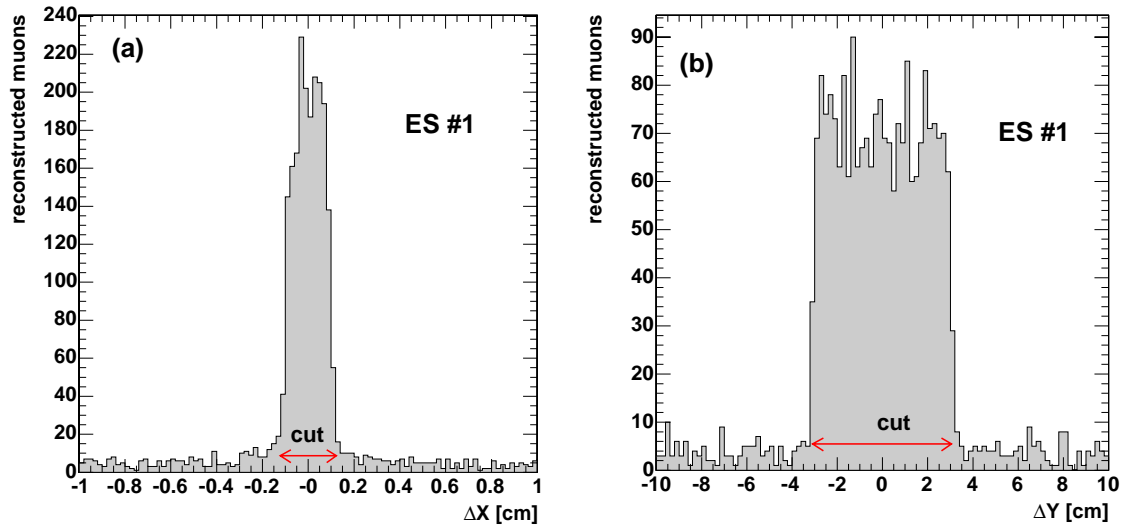


Figure 10.  $\Delta X$  (a) and  $\Delta Y$  (b) distance of track hits and coordinates of strips with signal for  $X$ -plane

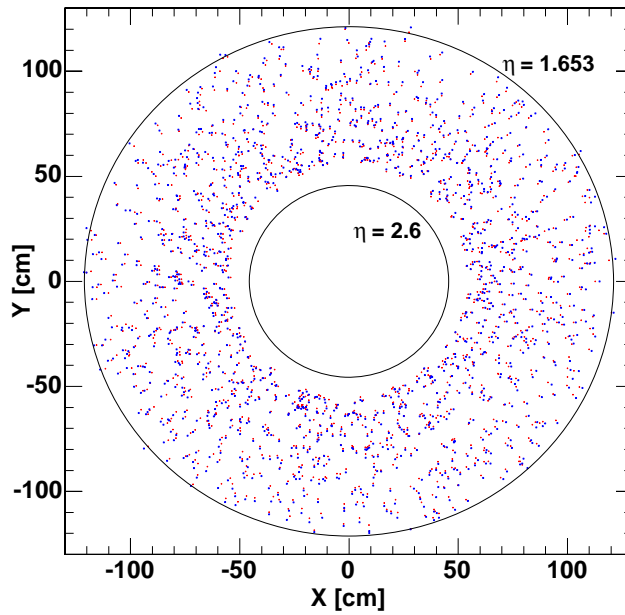


Figure 11. The hit profile for the accepted tracks on the Preshower (red:  $X$ -plane, blue:  $Y$ -plane)

The reconstruction of muon tracks is very good with a resolution  $\Delta p_T / p_T \cong 1.8\%$  (fig.12). In table 2 the results of the single muon sample analysis are summarized. About 58% of the tracks pointing to the ES fiducial region pass all cuts and selection criteria and contribute to the MIP distributions. Overall efficiency is about 17% of all muon tracks in the full CMS acceptance region for a flat pseudorapidity distribution.

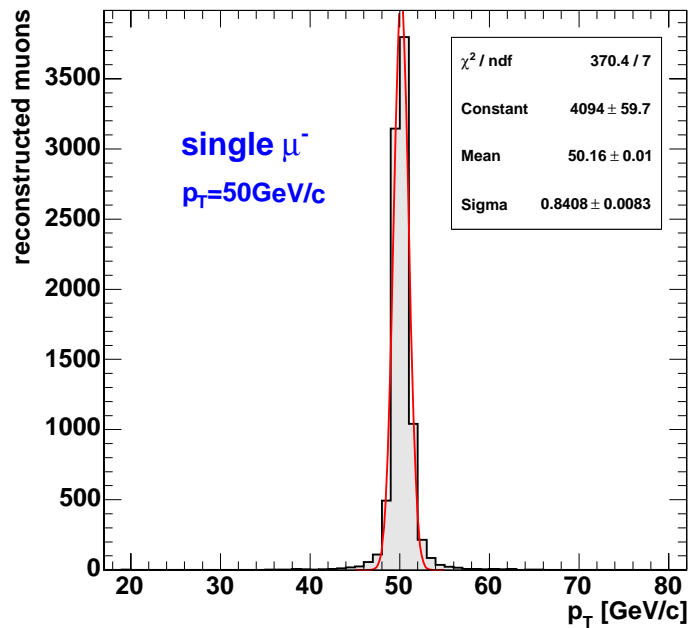


Figure 12.  $p_T$  distribution of reconstructed tracks for single  $\mu^-$  with  $p_T=50\text{GeV}/c$

Total Events (single tracks), flat $ \eta  < 2.6$	10000
Total reconstructed muon tracks, $ \eta  < 2.6$	9156 (91.6%)
Total tracks on Preshower region	2904 (29.0%)
Tracks surviving $\chi^2$ cuts	2092 (20.9%)
Tracks with matched signal strips (MIP distribution)	1675 (16.7%)

Table 2. Statistics of muon selection in single track events on both Preshower endcaps

The signal distributions of the selected muons for the two ES layers (ES #1 and ES #2) are shown in fig.13. These are the “MIP distributions” beneficial for calibration. The fit of Gaussian convoluted Landau distributions give “most probable values”, MP of  $87.1 \pm 0.9$  and  $84.6 \pm 1.0$  keV for the two layers respectively. This is in good agreement with the expected  $dE/dx$  (i.e. 87-94 keV) [12] of high energy muons for  $300 \mu\text{m}$  thick silicon and impact angles on the ES plane of  $10^0$ - $20^0$  increased by the “wedge angle” of the silicon sensors tilted with respect to the ES plane by  $3.8^{\circ}$ <sup>2</sup>. Note that the silicon sensors are not placed in radial arrangement on the ES disks with respect to the beam axis but rather parallel (the strips are vertical for the first layer, see fig.1b, and horizontal for the second). Also each sensor is placed on wedge-shaped aluminum tiles to ensure overlapping, thus resulting in an inclination angle with respect to the ES plane (i.e. the “wedge angle” mentioned above) [1].

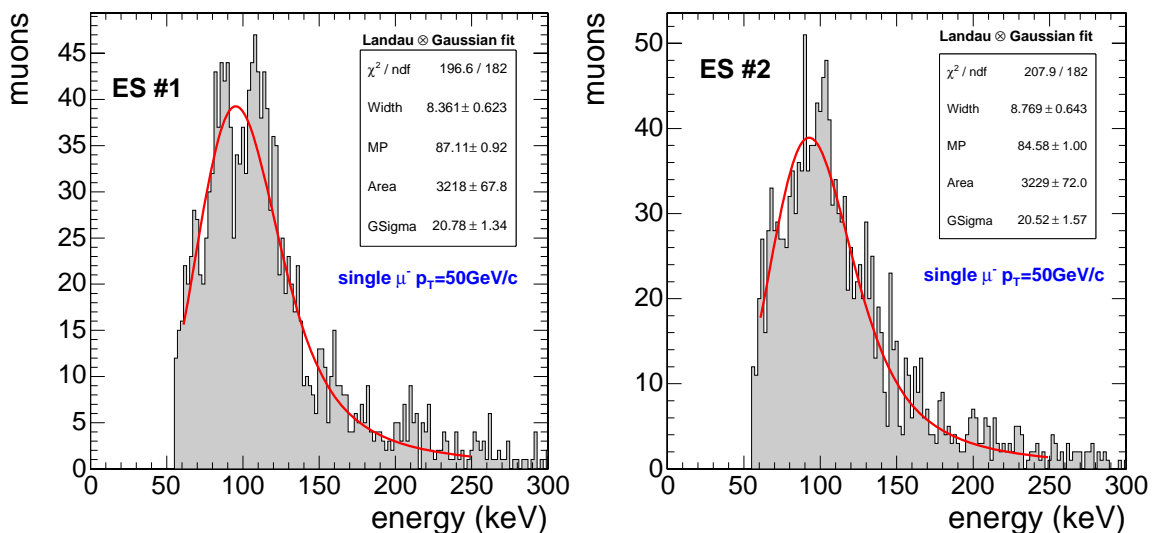


Figure 13. The signal distributions for the two layers of Preshower with single muon events.

The next step was to use full events with pileup as expected for the initial LHC luminosity of  $2 \times 10^{33} \text{ cm}^{-2} \text{ s}^{-1}$ . These event samples have at least one muon in the CMS acceptance region. The “GlobalMuonReconstruction” method is also used here to find and reconstruct the muon tracks as in the single muon events. The  $t\bar{t} \rightarrow \mu\mu + X$  for example is a high rate physics channel with a production cross section of  $\sigma = 5 \times 10^{-7} \text{ mb}$  and high probability to pass the HLT (High Level Trigger) requirements and be recorded. The tested events were generated with the Pythia\_102 and CMKIN\_1\_0\_2 software packages, simulated with OSCAR\_2\_4\_5 [13] and digitized with ORCA\_7\_6\_1. Note that OSCAR is using Geant4 [14] for the detector simulation. The data set name is “mu03\_tt2mu” with owner “mu\_2x1033PU761\_TkMu\_2\_g133\_OSC”. Following the same analysis procedure as before the inclusive MIP distributions shown in fig.14 were obtained. The fit of Gaussian convoluted Landau

<sup>2</sup> If  $\theta_i$  is the impact angle of the particles to the Preshower plane (i.e. on a ring),  $\theta_w$  the wedge angle and  $d_s$  the nominal thickness of the sensor, the actual silicon thickness traversed by the particles  $d_a$  will vary between  $d_a(\text{max}) = d_s / \cos(\theta_i + \theta_w)$  and  $d_a(\text{min}) = d_s / \cos(\theta_i) \cos(\theta_w)$ , a variation of about 1.5%.

distributions give “most probable values” of  $87.0 \pm 0.9$  and  $85.8 \pm 1.0$  keV for the two layers respectively. As expected, these values are very similar to those obtained with single muons.

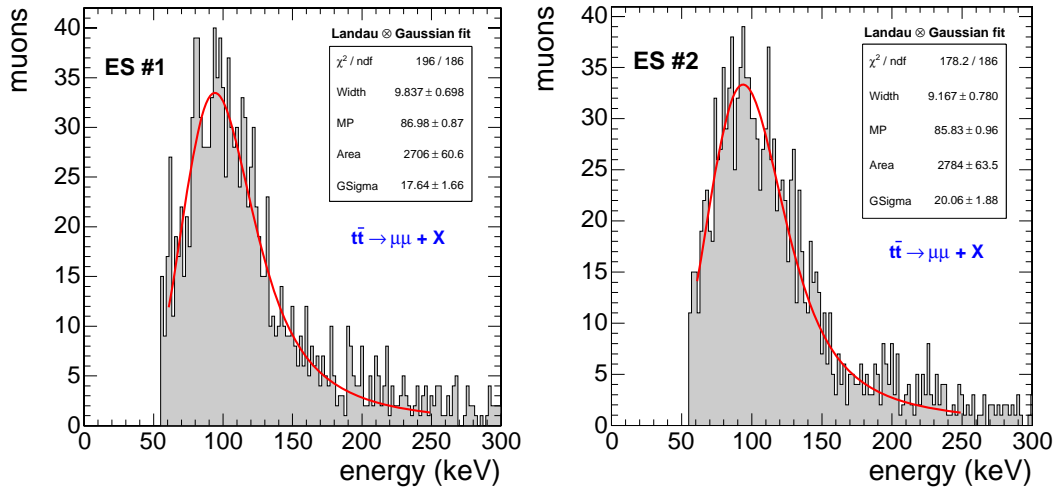


Figure 14. The signal distributions for the two layers of Preshower for  $t\bar{t} \rightarrow \mu\mu + X$  events.

The statistics of the  $t\bar{t} \rightarrow \mu\mu + X$  events sample are summarized in table 3. The final selection efficiency of the method to obtain the MIP distributions is about 18.8% of the total events or 51.1% of the muon tracks in the ES fiducial region. This event sample has two muons in the final state with  $p_T(\mu_1) \geq 20$  GeV/c and  $p_T(\mu_2) \geq 10$  GeV/c. The HLT requirements are:  $p_T > 19$  GeV/c for one muon and  $p_T > 7$  GeV/c for di-muon events at low luminosity [15].

Total $t\bar{t} \rightarrow \mu\mu + X$ events, pileup included	8000
Total reconstructed muon tracks, $ \eta  < 2.6$	17442
Total tracks on Preshower region	2943 (36.8% of events)
Tracks surviving $\chi^2$ cuts	2024 (25.3% of events)
Tracks with matched signal strips (MIP distribution)	1505 (18.8% of events)

Table 3. Statistics of  $t\bar{t} \rightarrow \mu\mu + X$  events

Then several other fully simulated event samples containing high energy muons were tested, such as  $Z/\gamma^*Z/\gamma^* \rightarrow \mu\mu\mu\mu + X$ , Drell-Yann  $DY \rightarrow \mu\mu$  or  $B_S^0 \rightarrow J/\Psi + \Phi$ , with  $J/\Psi \rightarrow \mu\mu$ . In all these samples the muon tracks selected for the MIP distributions are similar to those of the  $t\bar{t} \rightarrow \mu\mu + X$  events. The conclusion is that good MIP distributions can be obtained from any kind of muon events that pass CMS High Level Trigger, and are recorded on permanent storage. It should also be noticed here that with real data the “L3MuonReconstruction” method should be used instead of “GlobalMuonReconstruction”. This method reconstructs muons using CSC and RPC information (in the forward region) starting from Level-1 trigger seeds. The “L3MuonReconstruction” method is tested as well and the results were very similar compared to the “GlobalMuonReconstruction”.

## 7 The MIP distributions of pions

In addition to muons the feasibility of using pion tracks to obtain the MIP distributions was also examined. There will be plenty of low  $p_T$  pions in our detector mainly in minimum bias pileup events and jet events that pass the CMS HLT requirements. To start with, a representative sample of two-jet events with two gammas with

$p_T$  in the range of 50-170GeV/c was used, with low-luminosity pileup included. For the pion track reconstruction only tracker information is used, as explained in section 5, with the “CombinatorialTrackFinder” method. A low  $p_T$  cut is already applied in the reconstruction to remove spiral trajectories (accept tracks with  $p_T > 1.0\text{GeV}/c$ ). In our analysis code we used loose cuts (accept tracks with  $\chi^2/\text{ndf} < 2.0$ ) to increase statistics and followed the selection analysis the same way as for muons. The number of hits per track (a) and the  $\chi^2/\text{ndf}$  distribution (b) are shown in fig.15. The number of hits/track is below 17 and the  $\chi^2$  distribution is much broader with respect to muon tracks. Most of the tracks surviving the  $\chi^2$  cut have number of hits/track in the range of 10-16 thus eliminating the lower peak at 6 (fig.15a).

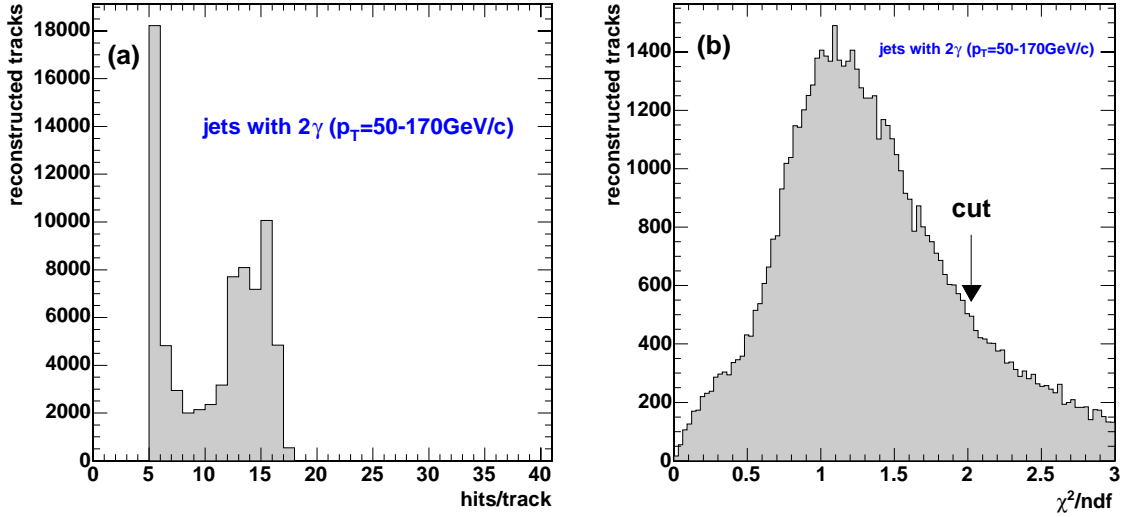


Figure 15. The number of hits/track and the  $\chi^2$  distribution of reconstructed tracks in the Tracker

Selecting the appropriate tracks for the MIP distributions, their corresponding hits on the two layers of ES are shown in fig.16. The pseudorapidity distribution of the accepted pions is not flat thus resulting in a concentration of hits at high pseudorapidity. In contrast to results obtained with muon tracks, there are also hits close to the ES limits of  $|\eta| > 2.6$ .

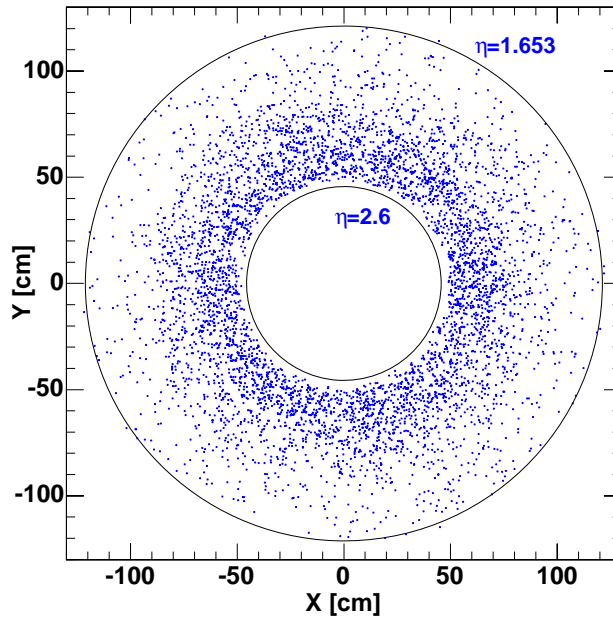


Figure 16. The hit profile of the Preshower layers for the accepted tracks

The signal distribution of the accepted tracks is shown in fig.17 for the two layers of the ES. The distributions are similar to those found with muons tracks. The fit of Gaussian convoluted Landau distributions give “most probable values” of the Landau peaks of 83.8 and 85.1 keV respectively for the first and second layer, with relative errors smaller than 1%.

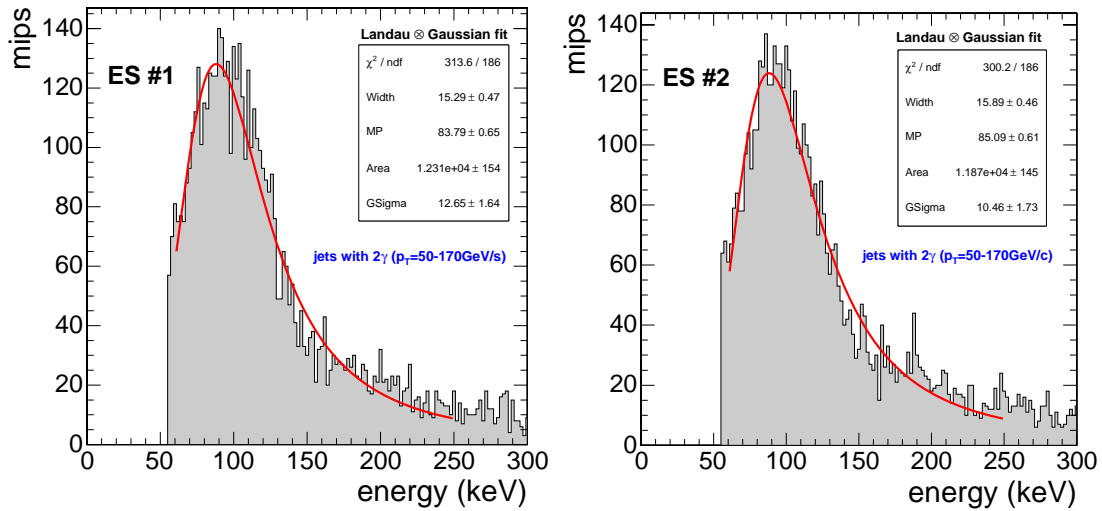


Figure 17. The signal distribution of the selected MIPs (mainly pions) for jet events

Then several pion event samples were tested including minimum bias events and single pion tracks of  $p_T=60\text{GeV}/c$ . The results are similar to those presented above. The statistics of the track selection is summarized for three representative event samples in table 4. There is a high rejection factor in MIPs at the last stage of selection (i.e. after the cut for the quality of the track reconstruction) which is of the order of 86% for the jet events and 93% for MB events. This is due to mismatch of the track hits on ES and strips with the signal, as a consequence of not completely perfect reconstruction of the low  $p_T$  pion tracks in Tracker and the strict cut of  $\Delta X$  (for  $X$ -plane, and  $\Delta Y$  for the  $Y$ -plane) on the strip pitch. This high rejection is characteristic of low  $p_T$  pions and is not seen in higher  $p_T$  pions, where the rejection factor at this stage is similar to muons (i.e. 15-20%, the last column of table 4).

	<b>Jets with <math>2\gamma</math></b> <b>(<math>p_T=50-170\text{GeV}/c</math>)</b>	<b>Minimum bias</b> <b>events</b>	<b>Single pions</b> <b>(<math>p_T=60\text{GeV}/c</math>)</b>
Total events	3500	6000	5000
Total reconstructed tracks, $ \eta  < 2.6$	271711	27416	3631
Total tracks on Preshower fiducial region	74064	8943	1217
Tracks surviving $\chi^2$ cuts	53208	7396	1020
Tracks with matched signal strips (the MIP distributions)	7549 (2.16MIPs/event)	489 (0.08MIPs/event)	870 (0.17MIPs/event)

Table 4. The selection statistics of three pion event samples

## 8 MIP distributions for different Preshower rings

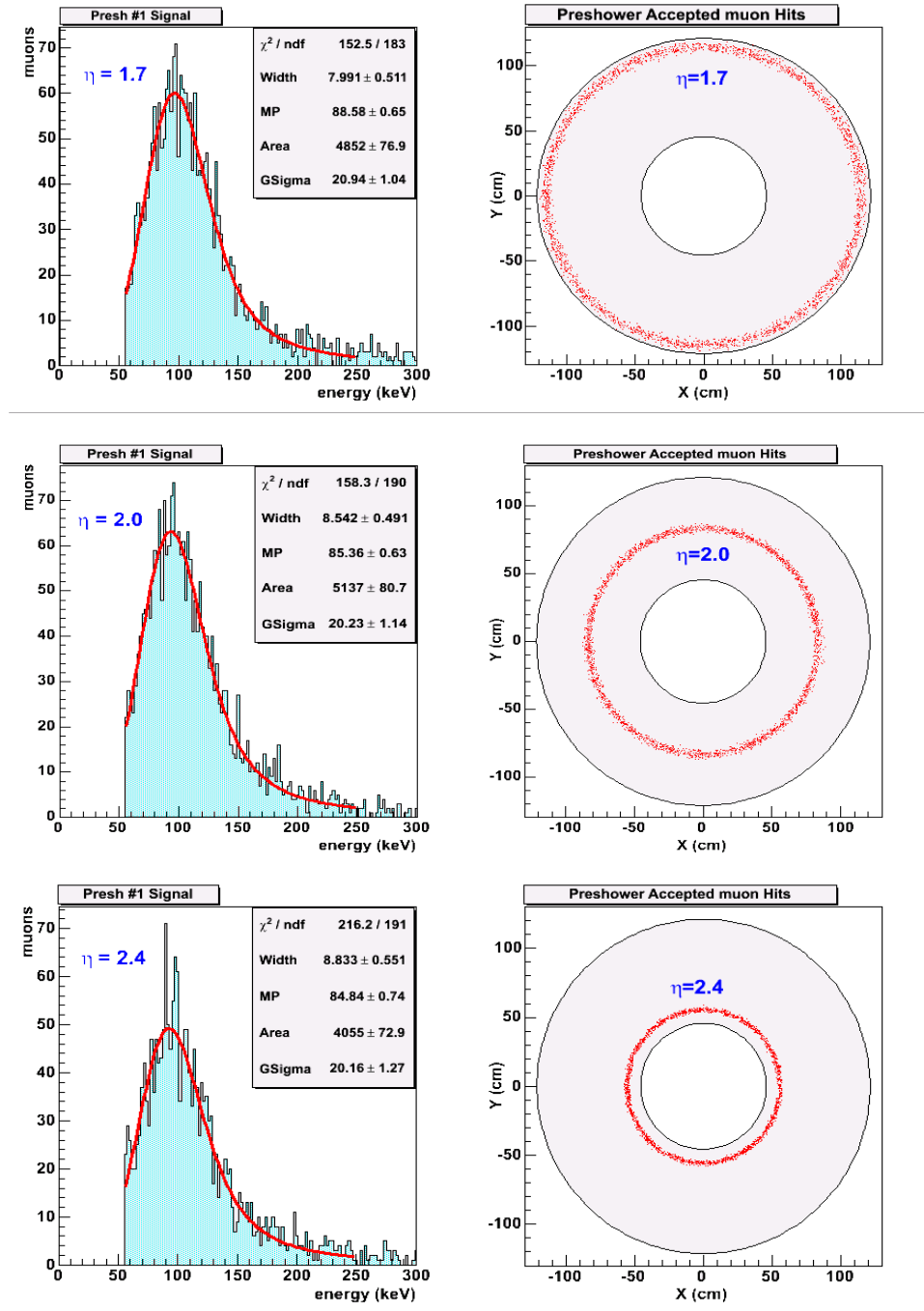


Figure 18. The MIP distributions of single muon samples ( $p_T=50\text{GeV}/c$ ) for three different Preshower pseudorapidities (i.e.  $\eta=1.7, 2.0$  and  $2.4$ ).

As shown in fig.1 the ES micromodules cover a disk area from pseudorapidity 1.653 to 2.6. Muons crossing these micromodules at different pseudorapidities will result in slightly different MIP distributions, due to the different thicknesses of silicon traversed (i.e.  $\Delta\theta \sim 10^0$  or  $\Delta(dE/dx) \sim 5\%$ ). In order to examine this effect three event samples with single muons of  $p_T=50\text{GeV}/c$  and pseudorapidities at primary vertex of  $\eta=1.7, 2.0$  and  $2.4$  were produced. These pseudorapidities correspond to impact angles of about  $20^0, 15^0$  and  $10^0$  respectively. The contribution of the “wedge angle” of each sensor with respect to the ES plane should also be added, thus resulting in a variation of the “effective thickness” of the sensors at the same ring by a factor of 1.5%. The full CMS simulation framework (CMKIN\_3\_2\_0, OSCAR\_3\_3\_0 and ORCA\_8\_2\_0) was used for the detector



simulation and reconstruction. The results of the evaluation of these samples are shown in fig.18. In the same figure next to MIP distributions the hit profile of the recorded muons on the ES fiducial area is shown. The MIP distributions are fitted with Gaussian convoluted Landau distributions and give “most probable values, MP” at 88.6, 85.4 and 84.8keV respectively for the three pseudorapidities mentioned. The difference in the energy deposited by particles with impact angle  $10^0$  with respect to those with impact angle  $20^0$  is expected to be of the order of 5% by calculating the thickness of the sensors. With the above MP values a difference of 4.2% is obtained which is in good agreement with the expected calculations.

## 9 Performance of the MIP calibration method

As mentioned before, the purpose of the present work is to find an effective method to calibrate the ES micromodules during the initial run of the CMS experiment at LHC and maintain it over the years to correct for the potential radiation damage of the micromodules, which leads to reduced charge collection efficiency. The position of the peak of our selected MIP sample energy has a linear sensitivity to a possible charge collection efficiency drop (i.e. reduction by 1 to 5%). This is justified by deliberately applying a “damage factor” of 0.99,...,0.95 to the signal response of each micromodule. Single muons with  $p_T=50\text{GeV}/c$  and  $\eta=2.0$  (fig.18, middle plots) were used for this study. In this way the resulting MIP distributions will be composed of signals from micromodules at the same ring, which experience similar radiation damage, and thus the same charge collection efficiency.

For each accepted track the signal output was distorted by a factor of 0.99,..., 0.95, with a Gaussian fluctuation of 1%, representing the charge collection efficiency due to the radiation damage over time. The new MIP distributions obtained are compared to the original one. The initial MIP distribution is shown on fig.19 (solid black line) and one of the corresponding MIP distributions (dashed red line) after 5% damage.

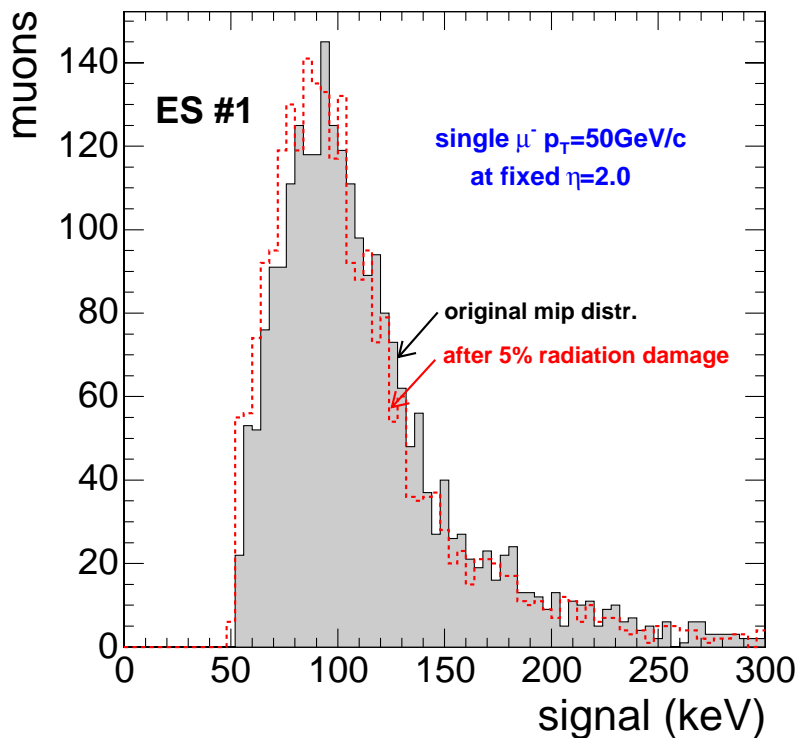


Figure 19. The expected MIP distributions before and after 5% radiation damage

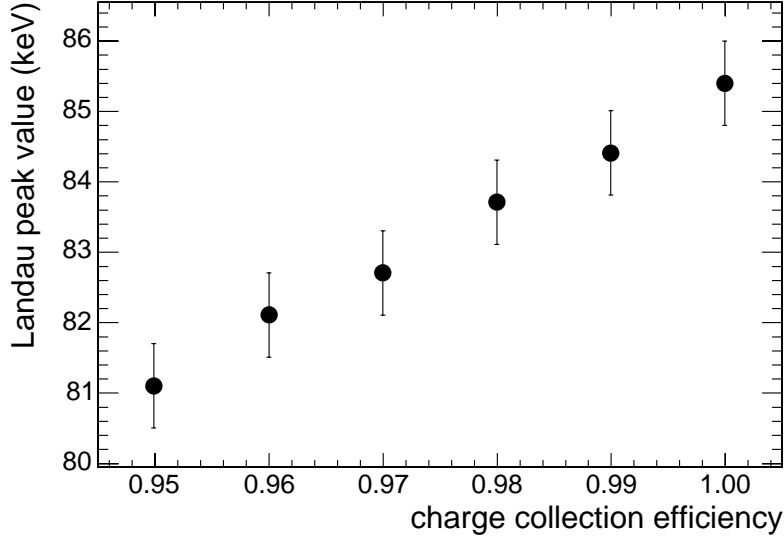


Figure 20. The peak value of MIP distributions as a function of the charge collection efficiency

The fit of Gaussian convoluted Landau distributions to the MIP distributions as before showed a displacement in the peak at lower values with consistent behaviour with linear dependence of the charge collection factors. The results are shown in fig.20 and summarized in table 5.

Charge Collection Efficiency	Landau Peak Value (keV)
1.00	85.4 ± 0.6
0.99	84.4 ± 0.6
0.98	83.7 ± 0.6
0.97	82.7 ± 0.6
0.96	82.1 ± 0.6
0.95	81.1 ± 0.6

Table 5. The damage factors (charge collection efficiency) and the corresponding peak values obtained

## 10 Time Required for MIP Calibration

In order to estimate the time needed for full ES calibration, the relative error on the MP value of Landau distribution was first calculated as a function of the distribution entries (fig. 21). It is found that with at least 800 MIPs collected the relative error is already at ~1%, which is well within the requirements. As mentioned above, with a flat pseudorapidity distribution of the MIP tracks the acceptance ratio is 1:7.4 for micromodules of the outer ring ( $|\eta| \sim 1.653$ ) of the ES compared to the micromodules in the inner ring ( $|\eta| \sim 2.6$ ) close to the beam-pipe. For example, if distributions with average entries 1800 per distribution are collected there will be micromodules in the outer region with about 800 MIPs/micromodule (just satisfying the requirements) and in the inner region with about 5900 MIPs/micromodule. There are about 4300 ES micromodules but one single MIP track will be used on both planes ( $X$  and  $Y$ ). This means that collecting 2150 distributions each by 1.8k MIPs on average (=3.9M) will be more than enough for the calibration purpose.

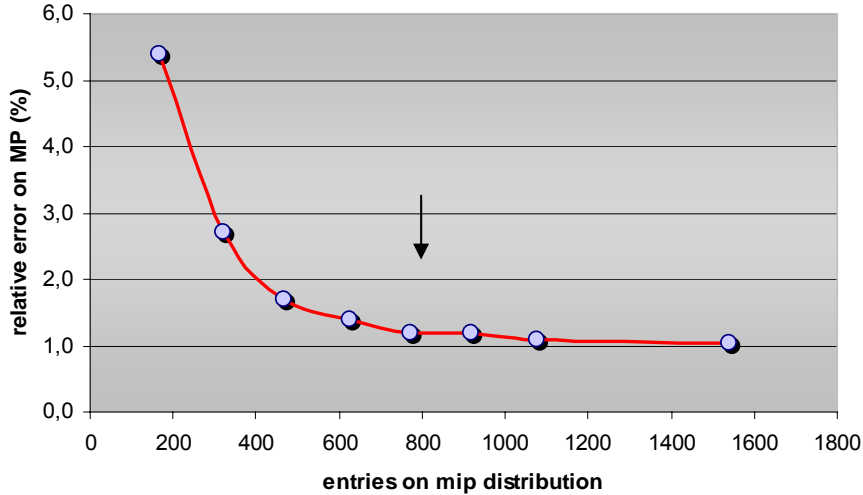


Figure 21. Relative error of Landau MP values as a function of entries in MIP distribution

At the initial LHC luminosity of  $2 \times 10^{33} \text{ cm}^{-2} \text{ s}^{-1}$  it is expected to have a machine duty cycle of at least 8 hours/day [16]. If only muons are used with an inclusive HLT rate to permanent storage of at least 25Hz [15] and a collection efficiency of our method of about 17% (table 2), it is estimated to have 120k selected muons per day (supposing flat  $\eta$  distribution). That means about a month is needed for collecting the full amount of MIPs required (i.e. 3.9M). The reconstruction of muon tracks is however limited to  $|\eta| < 2.4$ , which means that there will be very few MIP entries for the ES micromodules within  $|\eta| = 2.4 - 2.6$  (fig. 11). This problem can be avoided by using pions, as demonstrated previously. There will be plenty of minimum bias pileup events on storage (i.e. about 3 on average per event at low luminosity and about 18 at high luminosity) which contain mainly low  $p_T$  pions. It is shown above that for minimum bias events there is a selection efficiency for the described method of about 8% (Table 4). This means that for a permanent storage rate of events of  $\sim 100\text{Hz}$  we will have a  $\sim 300\text{Hz}$  total rate of minimum bias events and  $\sim 24\text{Hz}$  of pions selected for the MIP distributions. Following similar calculations as in the case of muons we end up with about a week of data taking for the total calibration. If also contributions of events like “jets with  $2\gamma$ ” are considered, which as shown above are a good source of pion tracks for our calibration method with high selection efficiency ( $\sim 2.1\text{MIPs/event}$ ), this time will be reduced to the order of even a few days without any compromise. Note that the calibration time should be minimized because, as explained in section 3, during the calibration the PACE3 will operate in HG mode, thus possibly saturating strip signals in the case of very high energy electromagnetic showers. For “nominal” LHC operation (i.e. at luminosity  $10^{34} \text{ cm}^{-2} \text{ s}^{-1}$ ) the time needed for calibration will be reduced by a small amount if only muons are used and by a factor of up to six if pions from pile-up events are used.

## 11 Summary

A method has been developed to obtain MIP distributions of muons and pions for *in-situ* inter-module absolute Preshower calibration to a  $\sim 1\%$  precision. This method was evaluated using fully simulated physics events at initial LHC luminosity and shows very promising results. The signal MIP distributions have distinct peaks that can be used to provide an absolute calibration. If only muons are used, the calibration time is estimated to be of the order of about a month. In the case of pions, the corresponding time will be much lower (no more than a week). A combined muon and pion track selection method will be the best solution for fast end effective Preshower calibration. A few days of data taking at the initial run of CMS at LHC startup luminosity of  $2 \times 10^{33} \text{ cm}^{-2} \text{ s}^{-1}$  will be sufficient. At the nominal luminosity of  $10^{34} \text{ cm}^{-2} \text{ s}^{-1}$  a time reduction by at least a factor two is expected.

## Acknowledgments

This work was partially supported by CERN-PH and GSRT (Greek General Secretariat for Research and Technology). I would like to thank D. Barney for his major help throughout this work, the CMS ECAL people, the University of Ioannina HEPLAB people, A. Kyriakis for his initial directions to the software framework ORCA, K. Kloukinas for his assistance and G. Daskalakis for the fruitful discussions and support at CERN.

## References

- [1] P. Wertelaers et al., CMS ECAL EDR-04, Volume 2: ECAL Preshower (ES), **2000-054**  
<https://edms.cern.ch/document/115565/2/TAB3>  
M. Della Negra et al., CMS Physics Technical Design Report Volume I: Software and Detector Performance, CERN-LHCC-**2006-001**  
<http://doc.cern.ch/archive/electronic/cern/preprints/lhcc/public/lhcc-2006-001.pdf>
- [2] Results from the 1999 Beam Test of a Preshower Prototype, P. Aspell et al., CMS-Note **2000-001**
- [3] P. Aspell et al., “PACE3: A large dynamic range analog memory front-end ASIC assembly for the charge readout of silicon sensors”, presented at the IEEE Nuclear Science Symposium & Medical Imaging Conference, October 23-29, 2005, Puerto Rico.
- [4] G. Minderico et al., “A CMOS low power, quad channel, 12-bit, 40MS/s pipelined ADC for applications in particle physics calorimetry”, presented at the 9<sup>th</sup> Workshop on electronics for LHC, Amsterdam 29 Sept–3 Oct 2003, Proceedings at <http://lhc-electronics-workshop.web.cern.ch/>
- [5] K. Kloukinas et al., “K-chip: A Radiation Tolerant Digital Data Concentrator chip for the CMS Preshower Detector”, presented at the 9<sup>th</sup> Workshop on electronics for LHC, Amsterdam 29 Sept–3 Oct 2003. Proceedings at <http://lhc-electronics-workshop.web.cern.ch/>
- [6] The DCU chip User Manual, G. Magazzu et al,  
[http://hep.fi.infn.it/CMS/TIB\\_integration/DCUF\\_User\\_Manual\\_v3.0.pdf](http://hep.fi.infn.it/CMS/TIB_integration/DCUF_User_Manual_v3.0.pdf)
- [7] P. Bloch et al., “Performance of Si sensors irradiated to  $5 \times 10^{14}$  n/cm<sup>2</sup>,” Nucl. Instrum. and Methods **A517** (2004) 121–127.
- [8] P. Kokkas et al., Detection of muons at 150 GeV/c with a CMS Preshower prototype, Nucl. Instrum. and Methods **A** (2006), in press.
- [9] The design and development of the front-end electronics for the CMS Preshower detector. By P. Aspell (Lyon, IPN), CERN-THESIS-2001-023, Oct 2001
- [10] ORCA, Object-Oriented Reconstruction for CMS Analysis, <http://cmsdoc.cern.ch/orca>
- [11] The CMS software homepage, <https://cmsdoc.cern.ch/cms/cpt/Software/html/General/>
- [12] Review of Particle Physics, S. Eidelman et al., Physics Letters **B592**(2004)1-1109
- [13] OSCAR, Object Oriented Simulation for CMS Analysis and Reconstruction, <http://cmsdoc.cern.ch/oscar>
- [14] GEANT4 Collaboration, S. Agostinelli et al., “GEANT4: A simulation toolkit,” Nucl. Instr. and Methods **A506** (2003) 250–303.
- [15] CMS Collaboration, “The TriDAS Project Technical Design Report, Volume 2: Data Acquisition and High-Level Trigger,” CERN/LHCC **2002-26**
- [16] R. Bailey, “Commissioning the LHC machine”, Presented at the 11<sup>th</sup> Workshop on electronics for LHC, Heidelberg 12-16 Sept 2005. Proceedings at <http://www.lecc2005.uni-hd.de/>